ACS OMEGA

http://pubs.acs.org/journal/acsodf

Article

Nanocellulose from *Nata de Coco* as a Bioscaffold for Cell-Based Meat

Mark S. Rybchyn,* Joanna M. Biazik, James Charlesworth, and Johannes le Coutre

Cite This: *ACS Omega* 2021, 6, 33923−33931

Read Online

ACCESS | Metrics & More | Article Recommendations

ABSTRACT: The three-dimensional formation of bio-engineered tissue for applications such as cell-based meat requires critical interaction between the bioscaffold and cellular biomass. To explore the features underlying this interaction, we have assessed the commercially available bacterial nanocellulose (BNC) product from Cass Materials for its suitability to serve as a bioscaffold for murine myoblast attachment, proliferation, and differentiation. Rigorous application of both scanning electron microscopy and transmission electron microscopy reveals cellular details of this interaction. While the retention rate of myoblast cells appears low, BNC is able to provide effective surface parameters for the formation of anchor points to form mature myotubes. Understanding the principles that govern this interaction is important for the successful scaling of these materials into edible, commercially viable, and nutritious biomass.

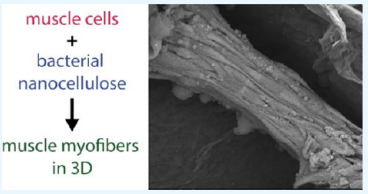

INTRODUCTION

Identification and characterization of materials for the purpose of using them as bioscaffolds is of significance in multiple ways and for different goals and applications. In all scenarios, a bioscaffold is being used to provide support for cellular growth at the surface. Multiple applications are being explored for novel bioscaffolds in the biomedical field for organ and tissue engineering applications. Over the past decade, interest is growing also in the food science field with the goal to use bioscaffolding for edible materials, most notably cell-based meat analogues.[1]

With a particular focus on these cellular agriculture applications, several scenarios are feasible, for which the right choice of bioscaffolding will be important, (i) The bioscaffold should not harm cells originating from the tissue of choice, for example, muscle cells. (ii) Ideally, the bioscaffold might be able to support growth and differentiation of the target cells in three dimensions. (iii) The scaffold is edible with potential nutritional benefits. (iv) The bioscaffold provides appealing organoleptic features, most notably texture and possibly taste and nutritional value as well. (v) The bioscaffold should not be animal based in origin. (vi) The bioscaffold should be relatively cheap to produce at a scale to compete with traditional meat production.

Currently, there is a clear need for bioscaffolds serving cellular agriculture purposes,[2] which can fit the above criteria. Several promising candidates are being investigated including chitin/chitosan,[3] recombinant collagens,[4] textured soy protein,[5] and of particular interest to this study, cellulose-based scaffold materials.[4] Some cellulose-based microcarriers have already been utilized for muscle cell cultures derived from embryonic chicken muscle.[6] Cellulose-based scaffolds can include decellularized plant tissue such as celery,[7] spinach,[8] or even grass.[9] However, plants are not the only source of cellulose for scaffold purposes, with acetic acid bacteria, such as the key genera of *Komagataeibacter*,[10] which is capable of producing cellulose from cheap source materials such as agricultural waste.[11,12] Cellulose derived from these bacteria commonly is referred to as bacterial nanocellulose (BNC). The primary difference between BNC and plant-based cellulose is the purity, with decellularized plant material also containing non-cellulose compounds such as lignins, sclerins, and other compounds.[13] Additionally, in comparison to BNC scaffolds, decellularized plant tissue generally requires harsher treatments to prepare.[14,15] The purity of BNC therefore lends itself toward further modification for scaffolding purposes.[14,15] BNC can be prepared into a variety of different forms, which include hydrogels, crystals, fibers, or pellets.[12,16] The variety of forms can lead to different applications of the material from use in proliferation for bioreactor systems to potential production of textured cuts of meat.

BNC is a material generally recognized as safe by the U.S. FDA,[12,14,17] which has been explored previously for cosmetic applications, such as the stabilization of emulsions[18] and biomedical applications such as wound repair for skin or corneal tissue, due to the biocompatible and wound healing properties.[18,19] One key application of BNC is the use as a scaffold material for tissue engineering, which has been

Received: September 21, 2021
Accepted: November 18, 2021
Published: December 1, 2021

explored for a number of applications including vascular tissue,[20] cartilage,[21] adipose tissue,[22] and neural tissue.[23] The variety of these applications showcase BNC as a biocompatible material in a cell culture context, indicating the potential for this material to be utilized for cell-based meat.

BNC has already been indicated for a number of potential applications in the food industry, potential supplementation of BNC has been investigated as a fat substitute in meatballs with 10% of fat being replaced with BNC while retaining similar organoleptic properties.[24] As BNC is a rich source of dietary fiber with cholesterol-lowering properties, it has been suggested as a potential ingredient in several food preparations such as biscuits or other products such as porridge.[25] Also of interest is the potential for BNC to be included in meat analogue products with the *Monascus* extract, suggested for the textural properties and cholesterol-lowering capabilities of the fiber.[12,26]

One key example of BNC use in food is the Filipino cuisine *nata-de-coco*, a dessert based on the production of BNC with coconut water, similar foods such as *nata-de-pina* or *nata-de-soya* can be produced from pineapple or soy, respectively.[25,27]

Given the evidence of BNC as a successful cell scaffold in biomedical contexts and the existing usage in the food industry, we explore the feasibility for BNC to fill the niche of a bioscaffold for cellular agriculture. In this study, we test the compatibility of the material with muscle cell attachment, proliferation, and differentiation using the established C2C12 muscle cell line.

RESULTS

Viable C2C12 Myoblasts are Retained by NBS Following Short-Term Incubation. C2C12 myoblasts were seeded directly on to nanocellulose bioscaffolds (NBS) (Figure 1) and incubated for 3 days. The number of myoblasts

Figure 1. Photograph of NBS that was used in the study. Photograph courtesy of Gary Cass (Cass Materials, Perth, Australia). Copyright 2021.

that were retained within the NBS (Figure 2, blue line) and cells that exited the NBS over the 3 day incubation period (Figure 2, red line) were quantified by the viability dye Cell Titer Blue (CTB) and total cell protein assay [bicinchoninic acid (BCA)]. Cell quantities obtained under these conditions were directly compared to numbers obtained on cell culture plastic as a known effective cell attachment substrate (Figure 2, black line). Saturation of cell culture plastic was reached at a plating density of ∼265 cells per mm^2 following 3 d incubation (Figure 2). When this number of cells was introduced into NBS (at 415 cells/mm^3), a significantly lower number of viable cells was retained compared to plastic (Figure 2A, $p < 0.0001$, black line *vs* blue line). In fact, a significantly higher number of viable cells was found to have exited NBS during the 3 day incubation period than was retained by NBS (Figure 2A, $p < 0.0001$, blue line *vs* red line). Total cellular protein (BCA) analysis (Figure 2B) was generally in agreement with the CTB data as myoblast saturation was again reached at 265 cells per mm^2 on cell culture plastic. However, at this cell density (equating to 415 cells/mm^3 NBS), BCA analysis showed that the number of cells retained within the matrix was not significantly different from cells that exited the material during the 3 day incubation (Figure 2B, ns, blue line vs red line). This likely represented cells that were not metabolically active and/or apoptotic, not contributing to the CTB signal, but were retained within the NBS.

Although NBS appears to be a relatively poor cell-binding substrate compared to standard cell culture plastic, viable cells are retained within NBS (Figure 2A). Both CTB and BCA quantification shows that increasing seeding cell density of NBS results in increased retained cell numbers within the scaffold (Figure 2A, $p < 0.001$ ### blue line; Figure 2B $p < 0.05$, #, blue line −25,000 *vs* 100,000 "cell # plated" in both cases), and at the highest cell density tested, the curve trend suggests that this was not yet saturated. By extrapolating our scaffold cell retention curves (Figure 2A,B blue lines), we conservatively infer that a cell seeding density of 1500 cells per mm^3 NBS would be suitable for longer term incubations to assess differentiation.

C2C12 Myotubes and Myoblasts Attach and Grow throughout the NBS Matrix. Scanning electron microscopy (SEM) was used to assess the characteristics of C2C12 cells that had attached, grown, and differentiated throughout the NBS matrix over a 1 month period following myoblast seeding at 1500 cells per mm^3 (determined in short-term experiments, as shown in Figure 2). Following incubation under differentiation conditions for 1 month, a general observation is that the cellular deposits attached to the NBS matrix exhibit a wide range of characteristics. Classic myotube formations of cylindrical shape are found within the NBS matrix away from the outer surface (Figure 3A i). However, more common types of cellular structures observed are groups of "flattened" myotubes in monolayers associated with undifferentiated C2C12 cells (Figure 3A ii). In some cases, these undifferentiated cells grow into amorphous cellular deposits of ∼50−100 cells on top of existing differentiated myotubes (Figure 3A iii). Although less common, in some instances larger, differentiated sheet-like structures are found within the NBS matrix, spanning up to 2 mm in diameter (Figure 4). Control NBS in the absence of seeded C2C12 cells is shown for comparison at several magnifications (Figure 3B).

1 month post seeding, viable cells are present within the NBS matrix, as confirmed via two simple observations. First, the phenol red in the culture media consistently turns from red to yellow, indicating media acidification upon cellular metabolism (Figure 5, top). Additionally, immediately following media change, the resazurin dye CTB was added to the media and soaked into the NBS. A visible light "blue-shift" upon reduction of the dye is indicative of cellular metabolic activity (Figure 5, bottom).

C2C12 Myotubes Directly Interact with NBS as Determined by EM Analysis. Transmission electron

https://doi.org/10.1021/acsomega.1c05235
ACS Omega 2021, 6, 33923−33931

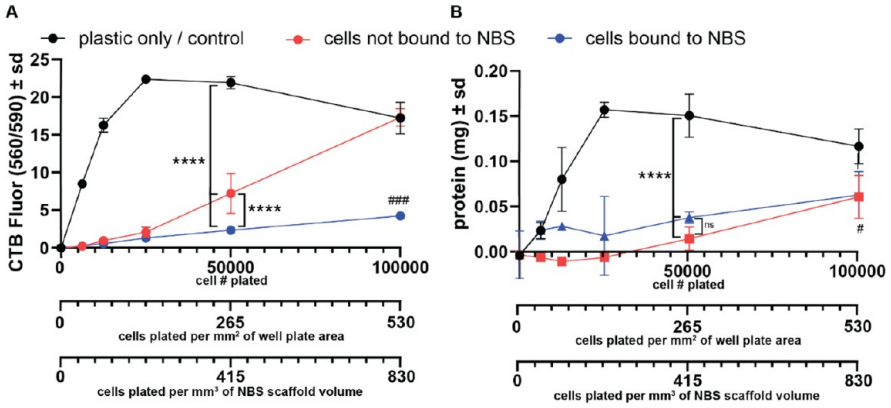

Figure 2. NBS was able to retain seeded myoblasts in 3 day cultures in a viable state. Myoblasts were seeded on to NBS at the indicated cell number, and following 3 days culture cell number was quantified by either (A) resazurin dye CTB or (B) total cellular protein, as determined by BCA assay. The response of cell quantification assays is shown as a function of the number of initially seeded cells (cell # plated), which is also expressed as the number of cells per mm^2 of cell culture plastic (cells plated per mm^2 of well plate area) and the number of cells per mm^3 of NBS (cells plated per mm^3 of NBS volume). Following 3 days incubation, myoblasts were quantified from the same well for cells within the NBS (blue line), and cells that had exited the NBS and bound to the cell culture plastic of the well plate (red line). Myoblasts seeded directly on to cell culture plastic in the absence of NBS (black line) served as a control, which was carried out independently in separate wells. "****" $p < 0.0001$, "###" $p < 0.001$, "#" $p < 0.05$, and "ns" not significantly different (two-way ANOVA, Tukey post-test, $n = 4$ biological replicates).

microscopy (TEM) was used to assess the ultrastructural characteristics of C2C12 cells that had attached, grown, and differentiated throughout the NBS matrix over a 1 month period (Figure 6). C2C12 cells are in direct contact with the NBS matrix after 1 month, as indicated by the close apposition of the C2C12 cell filopodia along the cell−matrix interface (Figure 6A−C). Cell filopodia were also observed by SEM analysis of the NBS matrix (Figure 7). TEM analysis showed that the general cell population exhibited a normal spindle-shaped morphology, which consisted of an organelle-rich cytoplasm, normal elongated mitochondria, and regular endoplasmic reticulum (ER), all indicative of viable cells (Figure 6A−C). Many of the cells within the matrix display an abundant population of lysosomes and other autophagic compartments (such as endosomes) (Figure 6D−F).

Prolonged Incubation for 2 Months of NBS Matrices with C2C12 Cells Results in a Withered Appearance of Cellular Material. When growth of C2C12 cells in NBS matrices is extended to 2 months, in many instances the cellular material appears to be withered and apoptotic by SEM (Figure 8) and TEM (Figure 9) analyses. Both differentiated myotube structures (Figure 8A) and amorphous cellular aggregates (Figure 8B) were found within the matrix with this appearance and likely were apoptotic or necrotic. Some amorphous cellular deposits contained both phenotypically normal cells and apoptotic cells exhibiting membrane blebbing (Figure 8C and inset). Apoptotic cells were irregular in shape, had an electron lucent cytoplasm, and exhibited membrane blebbing around the cell periphery by TEM analysis (Figure 9). Within these apoptotic cells, the mitochondria were round, electron lucent, and swollen, also suggesting cellular damage (Figure 9). We assume that it is unlikely this observed cell death was linked to nutrient deprivation from the media, which was changed regularly (every 2−3 days) or that it was due to a limitation of area to grow within the NBS matrix as a general observation from all SEM analysis was that the vast majority of the matrix was unoccupied by any cellular deposits.

DISCUSSION

The data presented support the proposal that BNC can serve as a functional support for skeletal muscle cell attachment and differentiation, an observation in alignment with previous studies.[6,28−30] However, in its unmodified form from Cass Materials, the commercially available product does suffer from low cell retention and thus would not serve as an efficient myoblast scaffold without further development.

Short-term studies showed that the BNC used in this study is only capable of retaining a small percentage of cells seeded, at least when compared to traditional cell culture plastic. Attempts to limit loss of cells from the matrix using small seeding volumes and giving cells an increased chance of binding nevertheless resulted in a majority of cells lost from the scaffold following seeding. Although this was a limitation of the scaffold, some viable cells were retained within NBS and therefore longer term differentiation studies were possible. To quantify the cellular material directly bound to the NBS matrix in longer term cultures, a punch biopsy was used to take several independent sections of NBS (~80 mm^3) containing cellular material following the 1 month incubation under differentiation conditions (or control sections without cells). Following extensive washing with isotonic saline, a BCA assay was used to quantify total cellular protein. By simultaneously assessing a suspension of C2C12 myoblasts of known density within the same BCA assay, an approximation for the cell number can be calculated from total cell protein data. Values obtained from replicate NBS sections were highly variable suggesting heterogeneity of cell distribution within the matrix. The mean value obtained was ~600 cells/mm^3 NBS section, corresponding to ~3.6×10^5 cells in the entire NBS section used for cell seeding at 1 month post seeding. This corresponded to ~10−20% of the original seeding number used (4500 cells/mm^3). The value of ~10−20% is in agreement with the values obtained from the shorter term experiments (Figure 2) and may simply be a limitation of the scaffold in terms of cell density.

This observation is important. Such low retention explains the general observation that although we did confirm differentiated cell structures within the matrix by SEM, these

https://doi.org/10.1021/acsomega.1c05235
ACS Omega 2021, 6, 33923−33931

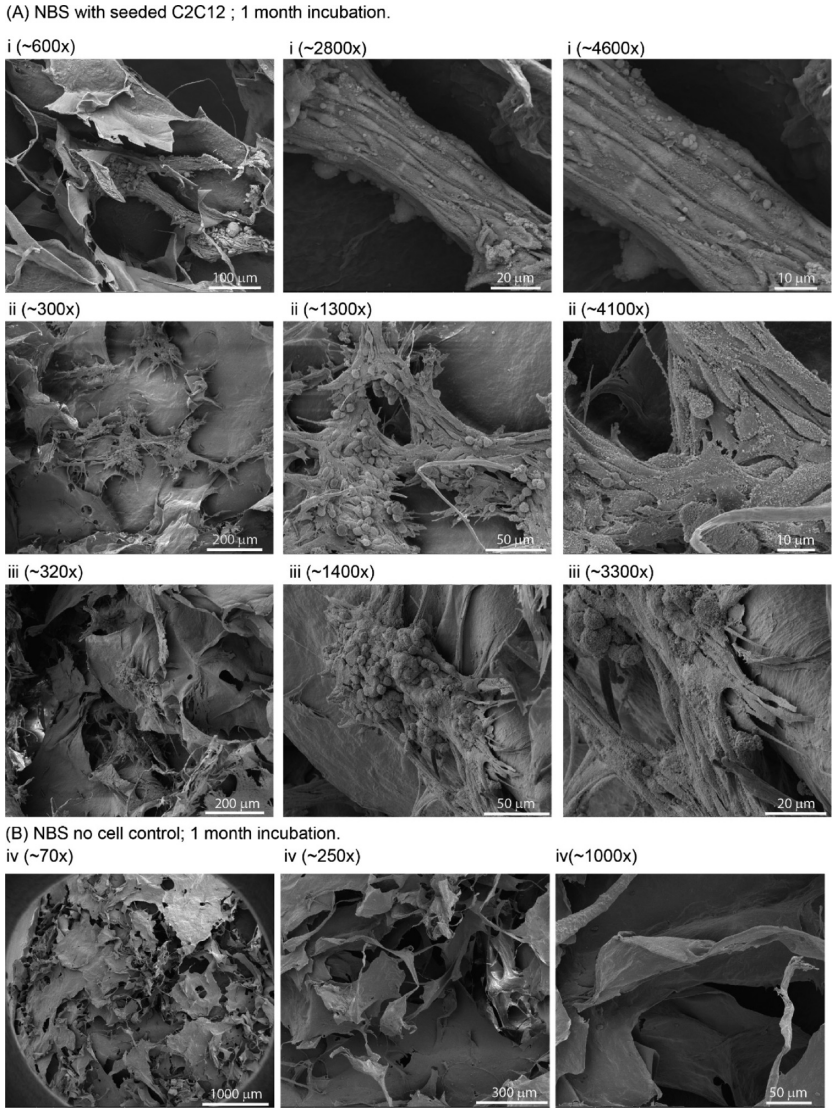

Figure 3. NBS as a functional support for myoblast attachment and differentiation to several distinct structural phenotypes. (A) SEM images of NBS that was seeded with C2C12 myoblasts and maintained for 1 month in 2% v/v HS to promote myoblast differentiation. SEM revealed several different types of cellular structures that were present within the NBS matrix. SEM shows (i) typical cylindrical myotube structures, (ii) myotubes in flattened cell monolayers that also contained undifferentiated mononuclear myoblasts on the monolayer surface, and (iii) monolayer structures that were associated with larger amorphous cellular deposits. (B) NBS maintained under the same conditions without cells at several magnifications. SEM magnifications used are shown as bracketed numbers above each image.

are not abundant and the vast majority of the NBS was unoccupied by cells when examined by SEM. While it is possible that cellular material is lost during the fixation process, it would seem likely that many of the sites within the NBS are not suitable as a cell-binding substrate. It is not clear why certain sites within the matrix enable cell interactions and others are unfavorable. However, given the chemical uniformity of BNC, it is possible that the sites where we observed cellular deposits were more sterically favorable for the seeded cells to access and bind.

There are several possible modifications that would likely improve cell binding. For example, modification of the surface hydroxyl groups of cellulose[31,32] or alignment of the BNC fibers have all been shown to be effective.[29] Pore size has also been linked to cell retention in a range of scaffolds, with a balance between having a pore size large enough for the exchange of nutrients and oxygen with smaller pores encouraging greater binding to the substrate.[33] The optimal pore size would have to be determined for specific cell type and material used. Specifically in the case of myoblasts, optimal pore size would also have to take into account the differentiation process to the much larger myotube/myofibril structure. Similarly, the BNC could be processed into different forms depending on use such as aligned nanowhiskers.[29] Another potential use of BNC is in hydrogels,[16,20] which can potentially be mixed with other compounds to enhance cell adhesion/proliferation,[34] mechanical properties such as texture,[35] or even nutrition.[36] A wide range of materials, including BNC, are being assessed for their suitability as bioscaffolds for cultured meat. For a comprehensive review of this field, please see a study by Seah et al.[37]

SEM identified several different differentiated cellular structures within the NBS matrix. Of interest was the finding that mononuclear myoblasts were abundant in a state bound to differentiated monolayer sheet structures. It is possible that these sheet structures are providing a favorable binding site for

https://doi.org/10.1021/acsomega.1c05235
ACS Omega 2021, 6, 33923−33931

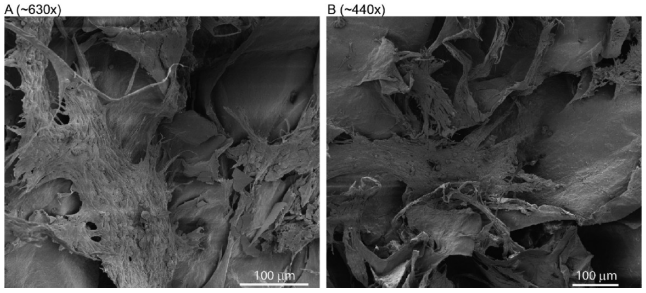

Figure 4. NBS was a functional support for myoblast attachment and differentiation into large differentiated monolayer sheets. (A,B) SEM images of NBS that was seeded with C2C12 myoblasts and maintained for 1 month in 2% v/v HS to promote myoblast differentiation. The two examples presented are from larger (up to 2 mm) differentiated monolayer sheets of myotubes that were present within the NBS matrix. SEM magnifications used are shown as bracketed numbers above each image.

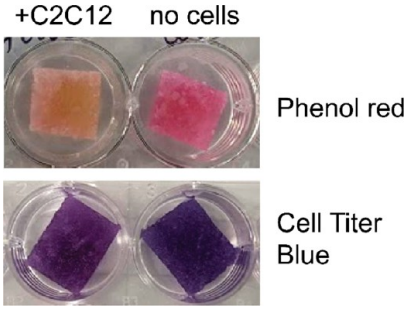

Figure 5. Viable cells were present in the NBS matrix following a 1 month incubation. Photograph of NBS scaffolds in individual wells of a 12 well plate at the end of a 1 month growth period following media aspiration. NBSs that were seeded with cells are shown on the left (+C2C12), and no cell controls are shown on the right (no cells). (Top) In cell seeded NBS, the pH indicator phenol red present in the growth media changed from red to yellow during the final 2−3 day media cycle due to acidification of the media by cellular metabolic activity. (Bottom) When the resazurin dye CTB was soaked in to replicate NBS in fresh media, a blue shift occurred over the next 1−2 h, indicating the presence of viable cells within the matrix. Photography by M. Rybchyn.

unbound, undifferentiated myoblasts residing within the matrix. This would suggest that sequential, multiple rounds of cell seeding could be the best approach when using BNC scaffolds allowing cells to differentiate and thus generating "new" binding sites for the next round of seeded cells, which would increase the cell-to-scaffold ratio of the final product. Optimizing the seeding interval of around 7−20 days would likely be most effective in this regard as prolonged incubation (2 months) resulted in necrotic/apoptotic cellular deposits.

Moreover, SEM identified amorphous cellular aggregates that had not differentiated into a myotube phenotype. These aggregates are often observed closely interacting with already differentiated cell monolayers. As a single cell suspension was used to seed the scaffolds, these aggregates formed either due to single cells preferentially accumulating in these areas or cell replication was occurring within the matrix to form these aggregates. It is unclear why these cells are subsequently unable to differentiate, and it is possible that some sort of steric hindrance makes this process unfavorable as clearly cell-to-cell contacts were present in these deposits.

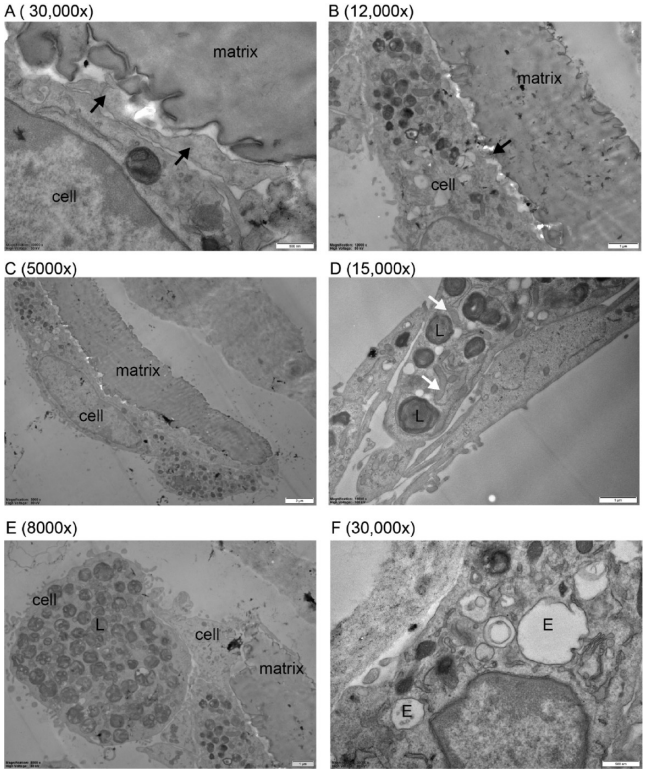

Figure 6. Ultrastructural analysis by TEM revealed that viable cells directly interacted with the NBS matrix. TEM images of cellular material bound to the NBS matrix after a 1 month incubation. (A−C) TEM images at several magnifications of the interaction sites between viable C2C12 cellular material (cell) and the NBS matrix (matrix). These interactions are facilitated by cell filopodia (black arrows). (D−F) Viable cells (cell) within the NBS matrix (matrix) generally exhibited a large population of lysosomes (L), endosomes (E), and normal elongated mitochondria (white arrows). TEM magnifications used are shown as bracketed numbers above each image.

It has been suggested that prolonged incubations of BNC can lead to greater proliferation and attachment due to secretion of various proteins by inoculated cells.[33] However, following prolonged incubation of cell seeded NBS, we observe that some of the differentiated cell structures adopt a withered appearance that likely represents necrotic or apoptotic cells. As the cells were never starved and media changes occurred regularly, this likely represents a normal progression of the differentiated skeletal cell phenotype after a prolonged period of *in vitro* incubation. One intriguing hypothesis could be that this might be due to the lack of either physical or physicochemical challenge provided to the myotube phenotype. Indeed, muscle tissue volume *in vivo* will decrease if not regularly challenged, and it seems plausible that this will also be a concern *in vitro*. The implications for clean meat are obvious. If prolonged growth periods are required to grow clean meat, then some kind of physiochemical stimulation of the differentiated muscle cell phenotype will likely be required or the texture and quality of the final product might deteriorate. Similar electrical stimulation has begun to be explored in relation to this concept for cellular agriculture purposes.[38]

CONCLUSIONS

Judging against our initial criteria for cellular agriculture scaffolds, NBS shows limited potential as a biocompatible

https://doi.org/10.1021/acsomega.1c05235
ACS Omega 2021, 6, 33923−33931

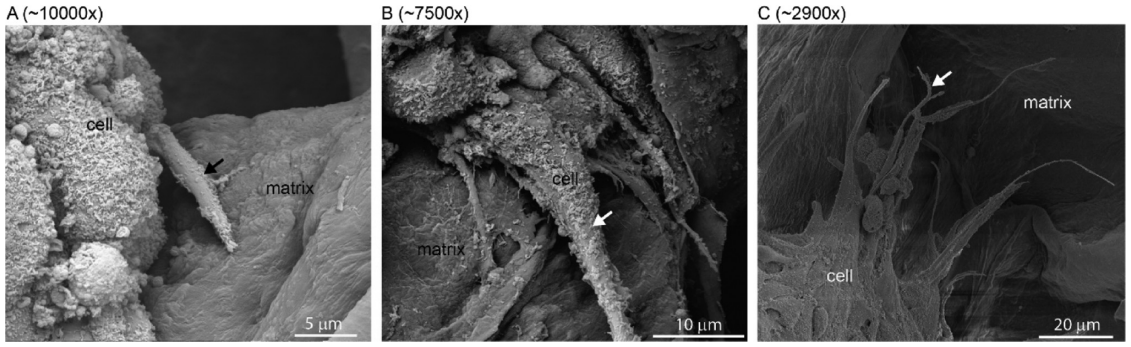

Figure 7. Cell filopodia facilitated the interaction between cellular material and the NBS matrix. (A−C) SEM images at several magnifications of cellular material (cell) bound to the NBS matrix (matrix) after a 1 month incubation. SEM analysis revealed the presence of cell filopodia facilitating the cell-to-matrix interaction (white and black arrows). SEM magnifications used are shown as bracketed numbers above each image.

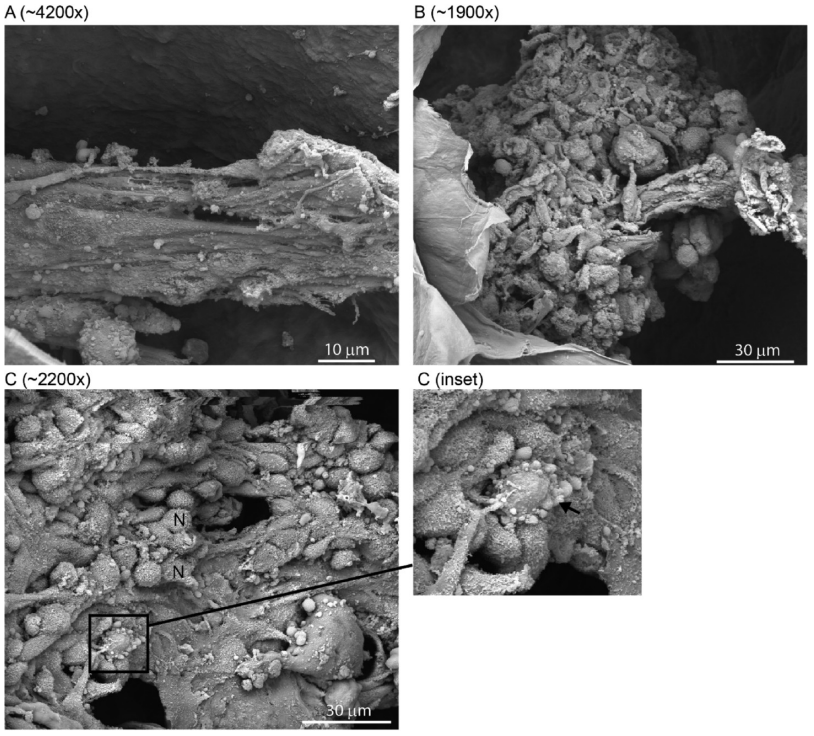

Figure 8. Prolonged incubation of NBS with C2C12 cells resulted in a withered and necrotic phenotype for cell structures. SEM images of NBS that was seeded with C2C12 myoblasts and maintained for 2 months in 2% v/v HS to promote myoblast differentiation. SEM shows that some of the components of cellular deposits including (A) myotubes, and (B,C) amorphous cellular deposits had adopted a necrotic and withered appearance within the NBS matrix following a prolonged 2 month incubation. (C) SEM shows that in some instances amorphous cellular aggregates contained both phenotypically normal cells (N) and apoptotic cells exhibiting membrane blebbing (inset, black arrow). SEM magnifications used are shown as bracketed numbers above each image.

matrix for cell-based meat, as evidenced by its ability to hold skeletal muscle cells in a viable state and permit their attachment and differentiation. However, BNC has already been indicated as a food safe substance with some nutritional benefit of dietary fiber.[39,40] Thus, to progress the type of NBS used in this study as a viable scaffold for cellular agriculture, alterations to the native state of the material will be required for characteristics such as pore size or available chemical moieties for cell binding.[34] In addition, the organoleptic properties of the final product could be modified to reach the desired texture. Only with such alterations, the scaffold will exhibit a binding capacity for cellular material that would result in a final product with a suitable cell-to-scaffold ratio for large-scale biomass production.

METHODS

Unless otherwise stated, all reagents were obtained from Merck KGaA (Darmstadt, Germany).

Cell Culture. The C2C12 mouse myoblast line was obtained from the European Collection of Authenticated Cell Cultures (ECACC). C2C12 cells were routinely maintained in DMEM containing 10% fetal calf serum (growth media) at 37 °C/5% CO_2 in a humidified incubator. Cells were routinely maintained at sub-confluent levels to prevent myoblast fusion. To promote differentiation to a myotube phenotype, C2C12 cells were instead maintained in DMEM containing 2% horse serum (HS) (differentiation media). Cells were routinely tested for the mycoplasma contamination (Ramaciotti Centre for Genomics, UNSW, Australia).

https://doi.org/10.1021/acsomega.1c05235
ACS Omega 2021, 6, 33923−33931

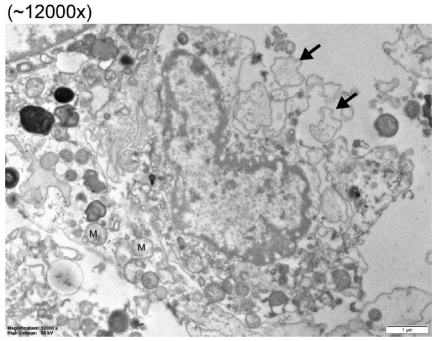

Figure 9. TEM analysis of the cellular material present following a prolonged incubation of NBS with C2C12 cells revealed apoptotic characteristics. TEM analysis showed that a large proportion of the cellular material present following a 2 month incubation were apoptotic by visual characterization. Apoptotic cells and their membranes were electron lucent, had round swollen mitochondria (M), and exhibited membrane blebbing (black arrows). TEM magnification was 12000×.

Nanocellulose Bioscaffolds. NBSs consist of BNC nanofibrils, that are produced by non-hazardous bacteria belonging to the acetic acid bacteria family, such as—but not limited to—*Komagataeibacter*, *Gluconacetobacter*, and *Acetobacter*. NBS were obtained from Cass Materials Pty Ltd. (Perth, Australia) in the sheet form and are marketed as a 3D cellulose matrix, which is both edible and biodegradable (Figure 1). NBS sheets (density <0.1 g/cm^3) comprise nanofibrils, ranging in diameter from 20 to 100 nm. Prior to the introduction of cellular material, BNC was washed extensively with PBS, pH 7.2, dried, and then autoclaved (121 °C/15 min) for sterilization.

Cell Seeding on NBS (Short-Term 3 Day Cultures for Cell Quantification). NBS sheets were cut to equally sized pieces with a biopsy hole punch (8 mm diameter), and replicates were placed in individual wells of a multiwell plate. Prior to cell seeding, all excess liquid from washing was removed from the material by aspiration so that it was in a semidried state. C2C12 myoblasts were trypsinized from standard cell culture plastic, triturated to a single cell suspension, and washed three times with media to remove excess matrix proteins present in the suspension. A single-cell suspension of C2C12 myoblasts was seeded at the various densities indicated for short-term experiments. Cells were seeded in a small media volume, such that it was able to be absorbed by the NBS material entirely in its semidried state without overflow. This was carried out to prevent cells exiting the material without having the opportunity to adsorb and attach to the NBS. Seeded NBS sheets were incubated for 2 h at 37 °C/5% CO_2 to permit cell attachment, prior to the addition of excess growth media for overnight incubation. Media-only negative controls were maintained on the same plates. Penicillin (100 U/mL) and streptomycin (0.1 mg/mL) were added to all media used on NBSs.

Cell Seeding on NBS (Long-Term 1−2 Month Cultures for SEM/TEM Analyses). NBS sheets were cut to an approximate size of $15(L) \times 15(W) \times 3(H)$ mm (~675 mm^3) and placed within a multiwell plate. Prior to cell seeding, all excess liquid from washing was removed from the material by aspiration so that it was in a semidried state. C2C12 myoblasts were trypsinized from standard cell culture plastic, triturated to a single cell suspension, and washed three times with media to remove excess matrix proteins present in the suspension. A single cell suspension of C2C12 myoblasts was seeded at a density of ~1500 cells/mm^3 onto NBS for longer term experiments. Cells were seeded in a small media volume, such that it was able to be absorbed by the NBS material entirely in its semidried state without overflow. This was carried out to prevent cells exiting the material without having the opportunity to adsorb and attach to the NBS. Seeded NBS sheets were incubated for 2 h at 37 °C/5% CO_2 to permit cell attachment, prior to addition of excess growth media for overnight incubation. For longer term cultures, the seeding process was repeated each day for a total of 3 days. Media only negative controls were maintained on the same plates. At day 5, media was replaced by differentiation media, which was changed every 2−3 day cycle for the course of the experiment. Some media discoloration generally occurred after every cycle indicating cell metabolic activity within the NBS matrix. Penicillin (100 U/mL) and streptomycin (0.1 mg/mL) were added to all media used on NBS.

CTB for Cell Viability. Cell Titer Blue (CTB) dye (Promega, WI, USA) was added directly to the media at the recommended concentration (10% v/v) and incubated for 2 h. Due to the highly porous nature of the NBS material, the dye was able to effectively diffuse throughout the entire NBS sheet and excess media when used to quantify cells attached to NBS. Where quantification of cells bound to NBS was performed, the scaffold was extensively washed in isotonic saline and moved to a new multiplate well prior to quantification to avoid signals from any cells that had exited the NBS and bound to the cell culture plastic. Fluorescence (Ex_{560}/Em_{590}) was measured using a CLARIOstar plate reader (BMG Labtech, Ortenberg, Germany).

Bicinchoninic Acid (Total Protein) Assay. NBS were extensively washed with isotonic saline, and then, cellular material was solubilized in PBS containing 1% v/v TX-100. A fixed volume of lysate or known concentration of bovine serum albumin was reacted according to BCA assay as per the manufacturer's instruction. Occasionally, to correlate protein concentration to cell number, a known number of C2C12 myoblasts lysed under the same conditions was also assessed by BCA simultaneously using the same fixed volume. Where quantification of cells bound to NBS was performed, the scaffold was always moved to a new multiplate well prior to quantification to avoid signals from any cells that had exited the NBS and bound to the cell culture plastic. Absorbances of the reacted samples were measured at 562 nm using a CLARIOstar plate reader.

TEM. NBS were fixed overnight at 4 °C in a fixative comprising 2.5% (w/v) glutaraldehyde in 0.2 M sodium phosphate buffer (pH 7.4). NBS were not washed prior to fixation. Fixed samples were rinsed with 0.1 M sodium phosphate buffer and post fixed in 1% osmium tetroxide in 0.2 M sodium phosphate buffer using a BioWave Pro + microwave tissue processor (Ted Pella, USA). After rinsing with 0.1 M sodium phosphate buffer, samples were dehydrated in a graded series of ethanol, infiltrated with resin (Procure, 812), and polymerized using an oven at 60 °C for 48 h. Ultrathin sections (70 nm) were cut using a diamond knife (Diatome) and collected onto carbon-coated copper slot TEM grids. Grids were post-stained using uranyl acetate (2% w/v) and lead citrate. Two grids were collected from duplicate regions for each sample and imaged using a JEOL 1400 transmission electron microscope (Tokyo, Japan) operating at 100 kV.

https://doi.org/10.1021/acsomega.1c05235
ACS Omega 2021, 6, 33923−33931

SEM. NBS were fixed overnight at 4 °C using a fixative containing 2.5% w/v glutaraldehyde in 0.2 M sodium phosphate buffer (pH 7.4). NBS were not washed prior to fixation. Fixed samples were then washed three times with 0.1 M sodium phosphate buffer followed by dehydration using a graded series of ethanol (30, 50, 70, 80, 90, and 100% v/v). Samples were then dehydrated using increasing concentrations of hexamethyldisilizane (HMDS) and left to air dry in a final 100% solution of HMDS. Duplicate regions from each sample were mounted onto SEM stubs, platinum coated and viewed using an FEI Nova NanoSEM 230 (Oregon, USA) operating at 5 kV.

Statistical Analyses. GraphPad Prism 9.2 was used for statistical analyses.

AUTHOR INFORMATION

Corresponding Author

Mark S. Rybchyn − *School of Chemical Engineering, University of New South Wales, Sydney, New South Wales 2033, Australia;* orcid.org/0000-0002-4336-6227; Email: m.rybchyn@unsw.edu.au

Authors

Joanna M. Biazik − *Electron Microscope Unit, Mark Wainwright Analytical Centre, University of New South Wales, Sydney, New South Wales 2033, Australia*

James Charlesworth − *School of Chemical Engineering, University of New South Wales, Sydney, New South Wales 2033, Australia*

Johannes le Coutre − *School of Chemical Engineering, University of New South Wales, Sydney, New South Wales 2033, Australia;* orcid.org/0000-0003-0781-216X

Complete contact information is available at: https://pubs.acs.org/10.1021/acsomega.1c05235

Funding

University of New South Wales, Sydney

Notes

The authors declare no competing financial interest.

ACKNOWLEDGMENTS

The authors acknowledge the generous gift of commercial BNC from Gary Cass (Cass Material, Perth, WA).

REFERENCES

(1) le Coutre, J. Editorial: Cultured Meat-Are We Getting it Right? *Front. Nutr.* **2021**, *8*, 675797.

(2) Ben-Arye, T.; Levenberg, S. Tissue Engineering for Clean Meat Production. *Front. Sustain. Food Syst.* **2019**, *3*, 46.

(3) Rubio, N.; Datar, I.; Stachura, D.; Kaplan, D.; Krueger, K. Cell-Based Fish: A Novel Approach to Seafood Production and an Opportunity for Cellular Agriculture. *Front. Sustain. Food Syst.* **2019**, *3*, 43.

(4) Campuzano, S.; Pelling, A. E. Scaffolds for 3D Cell Culture and Cellular Agriculture Applications Derived From Non-animal Sources. *Front. Sustain. Food Syst.* **2019**, *3*, 38.

(5) Ben-Arye, T.; Shandalov, Y.; Ben-Shaul, S.; Landau, S.; Zagury, Y.; Ianovici, I.; Lavon, N.; Levenberg, S. Textured soy protein scaffolds enable the generation of three-dimensional bovine skeletal muscle tissue for cell-based meat. *Nat. Food* **2020**, *1*, 210−220.

(6) Shainberg, A.; Isac, A.; Reuveny, S.; Mizrahi, A.; Shahar, A. Myogenesis on microcarrier cultures. *Cell Biol. Int. Rep.* **1983**, *7*, 727−734.

(7) Contessi Negrini, N.; Toffoletto, N.; Farè, S.; Altomare, L. Plant Tissues as 3D Natural Scaffolds for Adipose, Bone and Tendon Tissue Regeneration. *Front. Bioeng. Biotechnol.* **2020**, *8*, 723.

(8) Jones, J. D.; Rebello, A. S.; Gaudette, G. R. Decellularized spinach: An edible scaffold for laboratory-grown meat. *Food Biosci.* **2021**, *41*, 100986.

(9) Allan, S. J.; Ellis, M. J.; De Bank, P. A. Decellularized grass as a sustainable scaffold for skeletal muscle tissue engineering. *J. Biomed. Mater. Res., Part A* **2021**, *109*, 2471.

(10) Abol-Fotouh, D.; Hassan, M. A.; Shokry, H.; Roig, A.; Azab, M. S.; Kashyout, A. E.-H. B. Bacterial nanocellulose from agro-industrial wastes: low-cost and enhanced production by Komagataeibacter saccharivorans MD1. *Sci. Rep.* **2020**, *10*, 3491.

(11) Ruka, D. R.; Simon, G. P.; Dean, K. M. Altering the growth conditions of Gluconacetobacter xylinus to maximize the yield of bacterial cellulose. *Carbohydr. Polym.* **2012**, *89*, 613−622.

(12) Azeredo, H. M. C.; Barud, H.; Farinas, C. S.; Vasconcellos, V. M.; Claro, A. M. Bacterial Cellulose as a Raw Material for Food and Food Packaging Applications. *Front. Sustain. Food Syst.* **2019**, *3*, 7.

(13) Bar-Shai, N.; Sharabani-Yosef, O.; Zollmann, M.; Lesman, A.; Golberg, A. Seaweed cellulose scaffolds derived from green macroalgae for tissue engineering. *Sci. Rep.* **2021**, *11*, 11843.

(14) Shi, Z.; Zhang, Y.; Phillips, G. O.; Yang, G. Utilization of bacterial cellulose in food. *Food Hydrocolloids* **2014**, *35*, 539−545.

(15) Ludwicka, K.; Kaczmarek, M.; Bialkowska, A. Bacterial Nanocellulose-A Biobased Polymer for Active and Intelligent Food Packaging Applications: Recent Advances and Developments. *Polymers* **2020**, *12*, 2209.

(16) Athukoralalage, S. S.; Balu, R.; Dutta, N. K.; Roy Choudhury, N. 3D Bioprinted Nanocellulose-Based Hydrogels for Tissue Engineering Applications: A Brief Review. *Polymers* **2019**, *11*, 898.

(17) Sharma, C.; Bhardwaj, N. K. Bacterial nanocellulose: Present status, biomedical applications and future perspectives. *Mater. Sci. Eng., C* **2019**, *104*, 109963.

(18) Ludwicka, K.; Jedrzejczak-Krzepkowska, M.; Kubiak, K.; Kolodziejczyk, M.; Pankiewicz, T.; Bielecki, S. Medical and Cosmetic Applications of Bacterial NanoCellulose. In *Bacterial Nanocellulose*; Elsevier, 2016; pp 145−165.

(19) Anton-Sales, I.; D'Antin, J. C.; Fernández-Engroba, J.; Charoenrook, V.; Laromaine, A.; Roig, A.; Michael, R. Bacterial nanocellulose as a corneal bandage material: a comparison with amniotic membrane. *Biomater. Sci.* **2020**, *8*, 2921−2930.

(20) Sämfors, S.; Karlsson, K.; Sundberg, J.; Markstedt, K.; Gatenholm, P. Biofabrication of bacterial nanocellulose scaffolds with complex vascular structure. *Biofabrication* **2019**, *11*, 045010.

(21) Martínez Ávila, H.; Feldmann, E.-M.; Pleumeekers, M. M.; Nimeskern, L.; Kuo, W.; de Jong, W. C.; Schwarz, S.; Müller, R.; Hendriks, J.; Rotter, N.; van Osch, G. J. V. M.; Stok, K. S.; Gatenholm, P. Novel bilayer bacterial nanocellulose scaffold supports neocartilage formation in vitro and in vivo. *Biomaterials* **2015**, *44*, 122−133.

(22) Krontiras, P.; Gatenholm, P.; Hägg, D. A. Adipogenic differentiation of stem cells in three-dimensional porous bacterial nanocellulose scaffolds. *J. Biomed. Mater. Res., Part B* **2015**, *103*, 195−203.

(23) Innala, M.; Riebe, I.; Kuzmenko, V.; Sundberg, J.; Gatenholm, P.; Hanse, E.; Johannesson, S. 3D culturing and differentiation of SH-SY5Y neuroblastoma cells on bacterial nanocellulose scaffolds. *Artif. Cells, Nanomed., Biotechnol.* **2014**, *42*, 302−308.

(24) Lin, K. W.; Lin, H. Y. Quality Characteristics of Chinese-style Meatball Containing Bacterial Cellulose (Nata). *J. Food Sci.* **2004**, *69*, SNQ107−SNQ111.

(25) Dourado, F.; Leal, M.; Martins, D.; Fontão, A.; Cristina Rodrigues, A.; Gama, M. Celluloses as Food Ingredients/Additives: Is There a Room for BNC?. In *Bacterial Nanocellulose*; Elsevier, 2016; pp 123−133.

(26) Ullah, H.; Santos, H. A.; Khan, T. Applications of bacterial cellulose in food, cosmetics and drug delivery. *Cellulose* **2016**, *23*, 2291−2314.

(27) Iguchi, M.; Yamanaka, S.; Budhiono, A. Bacterial cellulose—a masterpiece of nature's arts. *J. Mater. Sci.* **2000**, *35*, 261−270.
(28) Bodin, A.; Bharadwaj, S.; Wu, S.; Gatenholm, P.; Atala, A.; Zhang, Y. Tissue-engineered conduit using urine-derived stem cells seeded bacterial cellulose polymer in urinary reconstruction and diversion. *Biomaterials* **2010**, *31*, 8889−8901.
(29) Dugan, J. M.; Collins, R. F.; Gough, J. E.; Eichhorn, S. J. Oriented surfaces of adsorbed cellulose nanowhiskers promote skeletal muscle myogenesis. *Acta Biomater.* **2013**, *9*, 4707−4715.
(30) Jia, B.; Li, Y.; Yang, B.; Xiao, D.; Zhang, S.; Rajulu, A. V.; Kondo, T.; Zhang, L.; Zhou, J. Effect of microcrystal cellulose and cellulose whisker on biocompatibility of cellulose-based electrospun scaffolds. *Cellulose* **2013**, *20*, 1911−1923.
(31) Courtenay, J. C.; Johns, M. A.; Galembeck, F.; Deneke, C.; Lanzoni, E. M.; Costa, C. A.; Scott, J. L.; Sharma, R. I. Surface modified cellulose scaffolds for tissue engineering. *Cellulose* **2017**, *24*, 253−267.
(32) Courtenay, J. C.; Sharma, R. I.; Scott, J. L. Recent Advances in Modified Cellulose for Tissue Culture Applications. *Molecules* **2018**, *23*, 654.
(33) Kirdponpattara, S.; Khamkeaw, A.; Sanchavanakit, N.; Pavasant, P.; Phisalaphong, M. Structural modification and characterization of bacterial cellulose-alginate composite scaffolds for tissue engineering. *Carbohydr. Polym.* **2015**, *132*, 146−155.
(34) Kabir, S. M. F.; Sikdar, P. P.; Haque, B.; Bhuiyan, M. A. R.; Ali, A.; Islam, M. N. Cellulose-based hydrogel materials: chemistry, properties and their prospective applications. *Prog. Biomater.* **2018**, *7*, 153−174.
(35) Shewan, H. M.; Stokes, J. R. Review of techniques to manufacture micro-hydrogel particles for the food industry and their applications. *J. Food Eng.* **2013**, *119*, 781−792.
(36) Qu, B.; Luo, Y. Chitosan-based hydrogel beads: Preparations, modifications and applications in food and agriculture sectors—A review. *Int. J. Biol. Macromol.* **2020**, *152*, 437−448.
(37) Seah, J. S. H.; Singh, S.; Tan, L. P.; Choudhury, D. Scaffolds for the manufacture of cultured meat. *Crit. Rev. Biotechnol.* **2021**, DOI: 10.1080/07388551.2021.1931803.
(38) Furuhashi, M.; Morimoto, Y.; Shima, A.; Nakamura, F.; Ishikawa, H.; Takeuchi, S. Formation of contractile 3D bovine muscle tissue for construction of millimetre-thick cultured steak. *NPJ Sci. Food* **2021**, *5*, 6.
(39) Jozala, A. F.; de Lencastre-Novaes, L. C.; Lopes, A. M.; de Carvalho Santos-Ebinuma, V.; Mazzola, P. G.; Pessoa-Jr, A., Jr.; Grotto, D.; Gerenutti, M.; Chaud, M. V. Bacterial nanocellulose production and application: a 10-year overview. *Appl. Microbiol. Biotechnol.* **2016**, *100*, 2063−2072.
(40) Corral, M. L.; Cerrutti, P.; Vázquez, A.; Califano, A. Bacterial nanocellulose as a potential additive for wheat bread. *Food Hydrocolloids* **2017**, *67*, 189−196.

https://doi.org/10.1021/acsomega.1c05235
ACS Omega 2021, 6, 33923−33931